How preparation and modification parameters affect PB-PEO polymersome properties in aqueous solution

Habel, Joachim Erich Otto; Ogbonna, Anayo; Larsen, Nanna; Krabbe, Simon; Almdal, Kristoffer; Hélix-Nielsen, Claus

Published in:
Journal of Polymer Science. Part B, Polymer Physics

Link to article, DOI:
10.1002/polb.24059

Publication date:
2016

Document Version
Peer reviewed version

How preparation and modification parameters affect PB-PEO polymersome properties in aqueous solution

JOACHIM HABEL[1,2], ANAYO OGBONNA[2], NANNA LARSEN[3], SIMON KRABBE[4], KRISTOFFER ALMDAL[5], CLAUS HÉLIX-NIELSEN[1,2,6*]

[1] Technical University of Denmark, Department of Environmental Engineering, Miljøvej, building 115, 2800 Kgs. Lyngby, Denmark

[2] Aquaporin A/S, Ole Maaløes Vej 3, 2200 Copenhagen, Denmark

[3] University of Copenhagen, Copenhagen Biocenter, Ole Maaløes Vej 5, 2200 Copenhagen, Denmark

[4] University of Copenhagen, Department of Biology, August Krogh Building, Universitetsparken 13, 2100 Copenhagen, Denmark

[5] Technical University of Denmark, Department of Micro- and Nanotechnology, Produktionstorvet, building 423, 2800 Kgs. Lyngby

[6] University of Maribor, Laboratory for Water Biophysics and Membrane Processes, Faculty of Chemistry and Chemical Engineering, Smetanova ulica 17, 2000 Maribor, Slovenia

Dated: March 21, 2016

ABSTRACT: The effect of formation and modification methods on the physical properties of polymersomes are critical for their use in applications relying on their ability to mimic functional properties of biological membranes. In this study we compared two formation methods for polymersomes made from polybutadiene-polyethylene oxide (PB-PEO) diblock copolymers: detergent-mediated film rehydration (DFR) and solvent-evaporation (SE). DFR prepared polymersomes showed a three times higher permeability compared to SE prepared polymersomes as revealed by stopped-flow light scattering (SFLS). SE prepared polymersomes broke down faster to structures < 50 nm diameter when processed with extrusion, which was more pronounced at 5 mg/ml, compared to 10, 20 and 25 mg/ml. Our results indicate that the bilayer of SE prepared polymersomes have a lower apparent fluidity. We also investigated the role of n-Octyl-β-D-glucopyranoside (OG) a detergent typically used for reconstitution of membrane proteins into lipid bilayers. Specifically, we compared dialysis and biobeads for OG removal to investigate the influence of these methods on bilayer conformation and polymer rearrangement following detergent removal. There was no significant difference found between method, temperature or time within each method. Our findings provide insight how biocompatible polymersome production affect the physical properties of the resulting polymersomes.

Keywords: PB-PEO, Polymersomes, Self-assembly, Film rehydration, Solvent evaporation, Detergent removal, Block copolymers

INTRODUCTION

Polymersomes, as a stable and versatile alternative to liposomes, are attracting increasing interest due to their ability to integrate and encapsulate a broad range of drugs and biomolecules[1–5], including water channel proteins to achieve highly selective biomimetic membranes for water separation[6–10]. Common for these vesicular systems is that they are based on the self-assembly of amphiphilic block copolymers.

The goal of this work is to analyze polymersome formation and modification in order to understand how these techniques can influence the polymersomes on the molecular level. Two formation approaches are compared: detergent-mediated film rehydration (DFR) and solvent evaporation (SE) with biocompatible organic solvents (methanol and acetone), minimizing potentially harmful effects on biomolecules. We analyze how formation methods influence polymersome osmotic permeability (P_f) and diameter (d_P). Where liposomes formed by FR, SE and electroformation have been compared[11], to our knowledge no compressive study exists which compares polymersome formation methods. Polybutadiene polyethylene oxide (PB-PEO) was chosen as a representative polymer for the polymersome monomer. PB-PEO is known to assemble to stable polymersomes, using FR[12].

Furthermore, we investigate two methods for detergent removal: polystyrene biobeads and dialysis and their impact on polymersome properties. For the detergent, n-Octyl-β-D-Glucopyranoside (OG) was selected, as far as it is one of the most common used detergents for membrane protein purification[13]. While there are several studies for detergent removal from liposomes[14–17], there are only few reports on detergent removal from polymersomes. Marsden et al. monitored PB-PEO polymersome d_P during OG-removal by dialysis, but with a qualitative rather than quantitative focus[18]. Kumar et al. studied how to optimize detergent removal rate in dialysis for PB-PEO polymersomes with high levels of incorporated aquaporin membrane proteins[19]. However, this approach only dealt with dialysis and was not focused towards the influence of individual parameters. Here we systematically analyze a series of polymers and this work can therefore be seen as a systematic approach towards the establishment of a framework for developing methods for industrial production of biocompatible polymersomes. We show how analytical methods like dynamic light scattering (DLS),

stopped-flow light scattering (SFLS) and freeze fracture transmission electron microscopy (FF-TEM) can be combined and used complementary in order to analyze polymersomes.

There are several methods for forming and modifying polymersomes. Formation methods can be subdivided into solvent-free methods and solvent-mediated methods following the principle of coacervation[20]. An overview over popular methods are summarized in Figure 1 and Table 1.

In solvent-free methods, the polymer in dry form is rehydrated with aqueous buffer. The convenient way is to use a polymer film referred to as FR, but also in powder or bulk form, polymers can be rehydrated (bulk rehydration). Optionally, voltage can be applied to release the polymer film from the wall instead of agitation as in the case of FR and bulk rehydration (electroformation). To achieve optimal conditions for the incorporation of membrane proteins, detergents can be added to the rehydrating buffer (DFR).

In solvent-mediated methods, the polymer is dissolved in a suitable organic solvent and mixed with aqueous buffer. This can be done dropwise (solvent injection) or in comparable volumes until a homogeneous phase is reached, whereafter the organic solvent has to be removed typically by SE.

With regard to polymer- or liposome size, vesicles formed with electroformation and SE are usually micrometer sized, whereas FR, bulk rehydration and solvent injection lead to nanometer sized vesicles with a significant polydispersity. In fact, many methods suffer from the formation of highly polydisperse or multilamellar polymersomes[21]. Another obvious problem of solvent-mediated methods and DFR is the remaining organic solvent and detergent. Remaining solvents are problematic for protein reconstitution whereas remaining detergent can lead to decreased polymersome stability.

The most efficient modification method against multilamellarity is freeze-thaw treatment[22], where combined extrusion and sonication help to achieve more monodisperse vesicles at the expense of stability[23]. The best choice for organic solvent removal is known to be dialysis[21]. The best detergent removal method is dependent on the detergent used. Every detergent has a specific concentration, above which detergent micelles can form, the so-called critical micelle concentration (cmc). For low cmc-detergents like Triton X-100 (0.37 mM[24], removal by biobeads is generally the best choice as it is difficult to dialyze micelles, whereas for high

cmc detergents (like n-octyl-β-D-glucopyranoside (OG) with 25 mM[24], used in this study), dialysis is typically sufficient[14].

This study consists of three parts: In the first part, PB_{29}-PEO_{16} polymersomes were formed using DFR and SE. d_P and permeability is measured using DLS and SFLS[25,26]. We use SFLS to analyze the kinetics of bilayer permeability by monitoring the change in light scattering during polymersome shrinkage induced by osmotically induced volume changes. PB_{29}-PEO_{16} has shown to produce robust polymersomes in a reproducible way, therefore it was mainly used for this part and the third part of the study.

The second part deals with the effect of polymer concentration and molecular weight (M_n) of the polymers on d_P and on resistance towards extrusion of SE formed polymersomes. The effect is measured using DLS. It is known that in some systems, d_P is increasing with increasing polymer concentration and that the latter in general also has a major influence in the resulting morphology of the self-assembly[27]. From an industrial point of view, polymer concentration is relevant when it comes to upscaling of production. Knowing the concentration regime, where the main assembling structure is still polymersomes and how polymersomes respond to processing steps like extrusion would be beneficial for biomimetic membrane research and technological applications. Measurements were done on four representative PB-PEO polymers, listed in Table 2.

The third part will compare two different detergent removal methods, dialysis and biobeads. With biobeads removal and dialysis, time and temperature were varied with PB_{29}-PEO_{16} as the exemplary polymer. Polymersome robustness and integrity after detergent removal is analyzed using two stress-tests: one consisting of excess addition of OG as a disruptive detergent[28]; and one consisting of a combination of excess NaCl at elevated temperature. The effects of the stress-tests are quantified using FF-TEM and DLS.

Table 1: Overview of all formation and modification methods for polymersomes and liposomes. Main challenges are polydispersity and lamellarity of the vesicles as well as removal of detergent or organic solvent. Abbreviations are given in the Abbreviations/Nomenclature section.

*Vesicle size depends upson water miscibility of organic solvent.

***Only valid for direct sonication, where an ultrasonic horn is put directly in the solution.

****Only achieved if vesicle size is exclusively bigger than pore size.

Method	Size scale	Advantages	Drawbacks	References	Amphiphiles used
Solvent-free formation methods					
Film rehydration (*film swelling*)	nm	Easy	Multilamellarity	[21,29,30]	[29]: PEE-PEO, PB-PEO
		No special equipment	Polydispersity		[21]: PMOXA-PDMS-PMOXA
Detergent-mediated film rehydration	nm	Biocompatible	Left detergent	[25]	[25]: PMOXA-PDMS-PMOXA
Film rehydration by	μm	Spontanity	Specialized equipment required	[30]	PBO-PEO
photolithography dewetting		Unilamellarity	Expensive		
		Control over vesicle size	Lowest vesicle diameter: 500nm		
Bulk rehydration	nm	Easy	Multilamellarity	[21,29]	[29]: PEE-PEO, PB-PEO
(*solid rehydration, bulk swelling*)		No special equipment	Polydispersity		[21]: PMOXA-PDMS-PMOXA
Electroformation (*Electroswelling*)	μm	Monodispersity	Specialized equipment required	[21,31,30]	Different polymers
			Defects in the layer		
			Low yield		
			Restriced to low M_w polymers		
Solvent-mediated formation methods					
Solvent injection (*Direct dissolution*)	nm	Minimal organic solvent left	Polydispersity	[21,32]	[32]: PS-PIAT
Solvent injection with inkjet	nm	Control over vesicle size	Hardly upscalable	[33]	P2VP-PEO
Solvent evaporation	nm/μm*	Fast & easy	Organic solvent still present	[21,34]	[34]: Lipids
(*Reverse-phase evaporation*)		High encapsulation	Polydispersity		
Microfluidic solvent evaporation	μm	Control over vesicle size	Specialized equipment required	[35,36]	[36]: P2VP-PEO, [35]: PLA-PEO
Modification methods					
Freeze thaw		High encapsulation	Hardly upscalable	[29,37,22,38]	[29]: PEE-PEO, PB-PEO
		Improves bilayer quality			[22,38]: Lipids
		Monolamellarity			
Sonication	nm	No material loss	Polydispersity	[22,29,39]	[22,39]: Lipids
		Robustness	Metal contamination**		
Extrusion	nm	Monodispersity***	Fragility	[29,39]	[29]: PEE-PEO, PB-PEO
Vortexing		Easy & fast	Hardly upscalable	[21]	
Dialysis		Monodispersity	Time consuming	[14,19]	[19]: PB-PEO
		Monolamellarity	High buffer volume		
Size exclusion chromatography		High efficiency	Polydispersity	[14]	[14]: Lipids
			High dilution		
Biobead removal		Fast	Potentially polymer adsorption	[14]	Lipids
Ultrafiltration	nm/μm	Mild	Potentially polymer removal	[21,40]	[40]: Lipids
Centrifugation	nm/μm	Fast	Hardly upscalable	[21,40]	[40]: Lipids

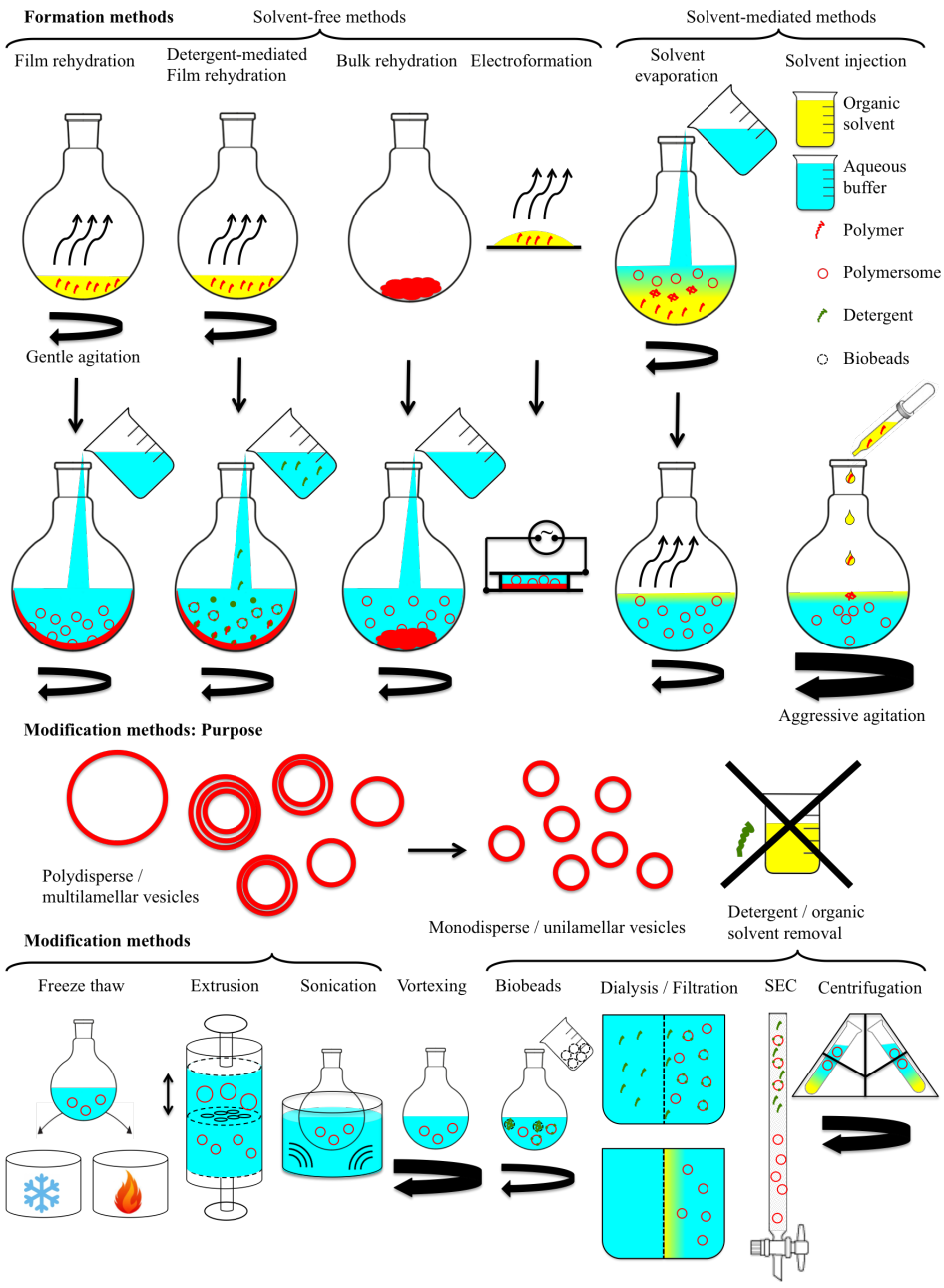

Figure 1: Schematic overview of polymersome formation and modification methods. The most common formation methods are film rehydration and electroformation for giant polymersomes. Further modification is mainly focused on achieving unilamellar and monodisperse polymersomes, as well as to remove detergent remaining organic solvent. Among modification methods, extrusion (unilamellar/monodisperse polymersome achievement) and dialysis (organic solvent removal) are the most used ones.

EXPERIMENTS

Materials

PB_{29}-PEO_{16}, PB_{46}-PEO_{32}, PB_{92}-PEO_{78} were synthesized via anionic polymerization following Förster[41]. PB_{43}-PEO_{32} was synthesized following a two-step-synthesis following Hillmyer[42]. Details to both syntheses are described elsewhere[43]. All polymers are listed in Table 2. They were characterized using NMR and SEC (Flow rate 0.5 ml/min). All other chemicals were purchased in analytical grade from Sigma-Aldrich, Brøndby, Denmark and used as received.

Table 2: Polymers used for this study. All values were determined using ^{1}H NMR analysis as described elsewhere[19]. M_n denotes number-mean molecular weight, PDI polydispersity index of the polymer length, defined as M_w/M_n and f hydrophilic volume ratio.

Polymer	$\mathbf{M}_n$ **[kg mol^{-1}]**	**PDI**	$\boldsymbol{f}$
PB_{29}-PEO_{16}	2.3	1.076	0.258
PB_{43}-PEO_{32}	3.75	1.110	0.316
PB_{46}-PEO_{32}	3.8	1.080	0.301
PB_{92}-PEO_{78}	8.4	1.167	0.344

Polymersome formation via SE

For polymer stock solutions, 25 mg/ml stock solution in acetone/methanol (9:1 (v/v)) were prepared. 2 ml of the stock solution were poured into a flask while gently stirred. A specific volume of Tris buffer (10 mM Tris pH 8.0, 50 mM NaCl) was added gently to the desired concentration, while continuing stirring for 30min. The organic solvent was then removed via evaporation on a Hei-VAP rotary evaporator (Heidolph, Schwabach, Germany) for at least 2 h at room temperature and 2 mbar at a rotation speed of 120 rpm until the majority of the organic solvent had been evaporated. Finally, the sample was extruded with track-etched polycarbonate membranes with pore sizes of 400 nm (Whatman, Maidstone, UK).

Polymersome formation via DFR

100 mg polymer was thawed, weighed and dissolved in 10ml $CHCl_3$ to get a 10 mg/ml solution. It was subsequently sonicated for 5min and stored at -20°C until use. 2.5 ml of the stock solution was injected in a 5 ml round flask and subsequently put on a Hei-VAP rotary evaporator (Heidolph, Schwabach, Germany) for at least 2 h at room temperature and 2 mbar at a rotation speed of 120 rpm to evaporate the $CHCl_3$. Then the polymer appearing as a smooth film on the flask wall was subsequently rehydrated with 200 μl of Tris buffer with 13 mg/ml OG and left stirring at least overnight at 22°C. It was diluted with 800 μl Tris buffer. For biobeads detergent removal, 20 mg biobeads were subsequently added and the sample was left on a shaker with 200rpm for 1 d, 2 d and 3 d at 4°C or 22°C. For dialysis detergent removal, samples were injected into a 1 ml Float-a-lyzer with molecular weight cut-off of 300 kDa (VWR, Herlev, Denmark) and put in a 500 ml beaker filled with Tris buffer while gently stirring. Samples were left in the beaker for 1 d, 3 d or 7 d, where the buffer was exchange twice a day.

Biobeads (Bio-Rad, Hercules, USA), are divinyl benzene cross-linked polystyrene beads with macroscopic pores, revealing a high overall surface area for the adsorption of organic material. The commonly used SM2 biobeads, used in this study are non polar and have a mean pore size of 90Å. The only adsorption force is hydrophobic bonding with no polar forces involved, as pH or ionic strength change seems not to influence the adsorption[14].

OG and T/NaCl stress treatment

For excess OG stress treatment (OGST) of FF-TEM samples, OG was weighed as a powder into a broad-edged 1.5 ml Eppendorf tube so that the final solution would have a concentration of 85 mg/ml following the addition of 100 μl sample. The solution was then vortexed for 5 s at 2500 rpm left stirring for 12 h before FF-TEM analysis. For DLS measurements, 900 μl of Tris buffer with 85 mg/ml OG was prepared in a broad-edged 1.5 ml Eppendorf tube. 100 μl of sample was added, vortexed and left stirring for 12 h until measurement. For temperature / NaCl stress treatment (TSST), NaCl was weight into a sharp-edged 1.5 ml Eppendorf tube to have a final concentration of 500 mM (dry NaCl for 450 mM plus 50

mM in the buffer). 100 μl of sample was mixed just before FF-TEM and set into a warming block with 95°C for 10 min. For DLS measurements, 100 μl of sample was added to 900 μl Tris buffer containing 500 mM NaCl and heated directly to 95°C for 10 min. Afterwards it was analyzed by DLS.

Analysis of d_P via DLS

DLS was performed with a Nano Zetasizer (Malvern, Worcestershire, UK). 1000 μl of sample were injected in a disposable cuvette and subsequently measured three times with 6 runs of 10 s per measurement at 22°C for the OG treatment samples and 70°C for the high temperature treatment samples. Raw data from light scattering was extracted from the volume particle size distribution that calculated using non-negative least square algorithm in order to minimize the bias towards larger polymersomes. Representative raw data can be found in the supplementary information.

Permeability measurements via SFLS

SFLS was measured with a SFLSM-300 (BioLogic, Claix, France) with a Xe-Hg lamp. The principle behind SFLS is a rapid mixing of the polymersome solution with an osmotic agent (usually NaCl or sucrose). The osmotic shock causes the polymersomes to shrink, resulting in increased light scattering measured at 90° using a photomultiplier tube. The scattering data was fitted to an exponential rise equation to calculate the water permeability of the bilayer P_f, using the following expression[25] :

$$P_f = \frac{k}{(S/V_0) * V_W * \Delta_{osm}} \tag{1}$$

where k is the rate constant of initial rise in the light scattering curve, S/V_0 the initial surface area to volume ratio of the vesicles, V_w the molar volume of water (18 cm^3 mol^{-1}) and Δ_{osm} difference in osmolarity[25]. 1M NaCl in Tris buffer was used as osmotic agent. 3 ml of 3 mg/ml PB_{29}-PEO_{16} polymersomes (for comparison of DFR and SE) and 10 mg/ml PB_{29}-PEO_{16}, PB_{43}-PEO_{32}, PB_{46}-PEO_{32}, PB_{92}-PEO_{78} polymersomes (for comparison of SE prepared polymers) was measured in a timeframe of 1.2 s during 8000 measurement points

at an excitation wavelength of 365 nm at a flow rate of 12 ml/s. 9 traces were averaged with BioKine software. Analysis and normalization of curves was performed with Excel, fitting was performed again with BioKine software (BioLogic, Claix, France).

Analysis of d_P and polymersome sturdiness via FF-TEM

FF was performed on a MED020 with EM VCT100 shuttle attached (Leica, Wetzlar, Germany). 1.2 μl of sample was injected into a 3 mm aluminium sample carrier at the side with 300 μm depth. Another sample carrier with the 200 μm depth was placed on top creating a sample volume where care was taken to avoid air bubbles. This sandwich was plunged into liquid ethane for 20 s and then immediately transferred to liquid N_2. The sample carrier was fixed at the sample holder and placed in a high vacuum chamber at -140°C. After the lower sample carrier had been removed, the sample was coated at the same temperature with 2 nm carbon layer, followed by 4nm platinum layer with 45° tilt and finally with a 19 nm carbon protection layer without tilt. Outside the chamber, the carrier was thawed for 5 min at 22°C. The carrier was then carefully placed at 45° angle into a 200 μl bath of Tris buffer with 100 mg ml^{-1} OG for 5 min for solubilizing the polymersomes in order to have them removed from the replica. Finally, the removed replica or single pieces of it were placed on uncoated TEM copper grids with 400 Mesh (Agar scientific, Essex, UK) that were as well carefully placed in the Tris/OG bath at 45°.

To minimize artifacts due to bad fracturing or fluctuations during the vitrification[43] that could lead to wrong conclusions in the determination of polymersome membrane sturdiness, two fractions of the replica of each of the three samples per conditions was placed on a TEM grid. Furthermore, different areas of each replica were observed, if the membrane sturdiness of the polymersomes could not be characterized clear enough in one area.

TEM observation of the replica was performed with a CM100 (Philips, Amsterdam Netherlands) with an installed Veleta 2k CCD camera (Olympus, Shinjuku, Japan). The applied voltage on a tungsten source was 80 kV with a 100 μm objective lense aperture. Analysis of d_P from the TEM images was performed by manual measurement via the image processing software Gimp (University of California, Berkeley, USA), using a correction factor of $4/\pi$ to balance out the error of d_P when the fracturing is not in equatorial plane[44].

RESULTS AND DISCUSSION

First we analyze the effect of polymersome preparation: SE versus DFR in terms of polymer size measured using DLS and polymersome stability using SFLS. Then we analyze the effect of polymer concentration for SE formed polymersomes. Finally we analyze the effects of dialysis versus biobeads for DFR formed polymersomes. Findings are discussed in terms of the issues involved in up-scaling production of polymersomes in the 100-200 nm d_P range.

Effect of preparation method

To investigate the role of preparation method, we prepared PB_{29}-PEO_{16} (3 mg/ml) polymersomes by DFR and SE respectively and extruded them through track-etched membranes with the aim to produced polymersomes in the 100-200 nm range. We assessed size distribution with DLS measurements of effective polymersome diameter presented as mean $\langle d_P \rangle \pm \delta$ where δ is the distribution width of d_P as obtained by non-negatively constrained least squares (NNLS) analysis[43].

The SE prepared polymersomes could not be pressed manually through the 200 nm track-etched membranes. Extrusion through 400 nm membranes led to polymersomes with $\langle d_P \rangle = 85 \pm 61$ nm and further extrusion through 200 nm membranes broke them down to structures with $\langle d_P \rangle < 50$ nm, most likely micelles (data not shown, as PB-PEO micelles are in the range of 15-40 nm[45], and we assume all structures < 40 nm to be micelles). These results indicate that once the formed polymersome bilayer are opened up by extrusion (at 400 nm) reveal a lower apparent fluidity so that they break down to smaller structures at 200nm. In contrast the DFR prepared polymersomes could be extruded through 200 nm directly, or through 400 nm and 200 nm afterwards yielding a $\langle d_P \rangle$ of 132 ± 60 nm without breaking down to smaller structures. This is also consistent with the difference in preparation procedure as the mixing time was much shorter with SE (some minutes) compared to DFR (at least 12h), so the bilayer had more time to reach an equilibrium structure. Thus it is possible to produce polymersomes with the faster SE method - however size may be difficult to control by extrusion. On the other hand if size control is important the slower DFR method is preferable.

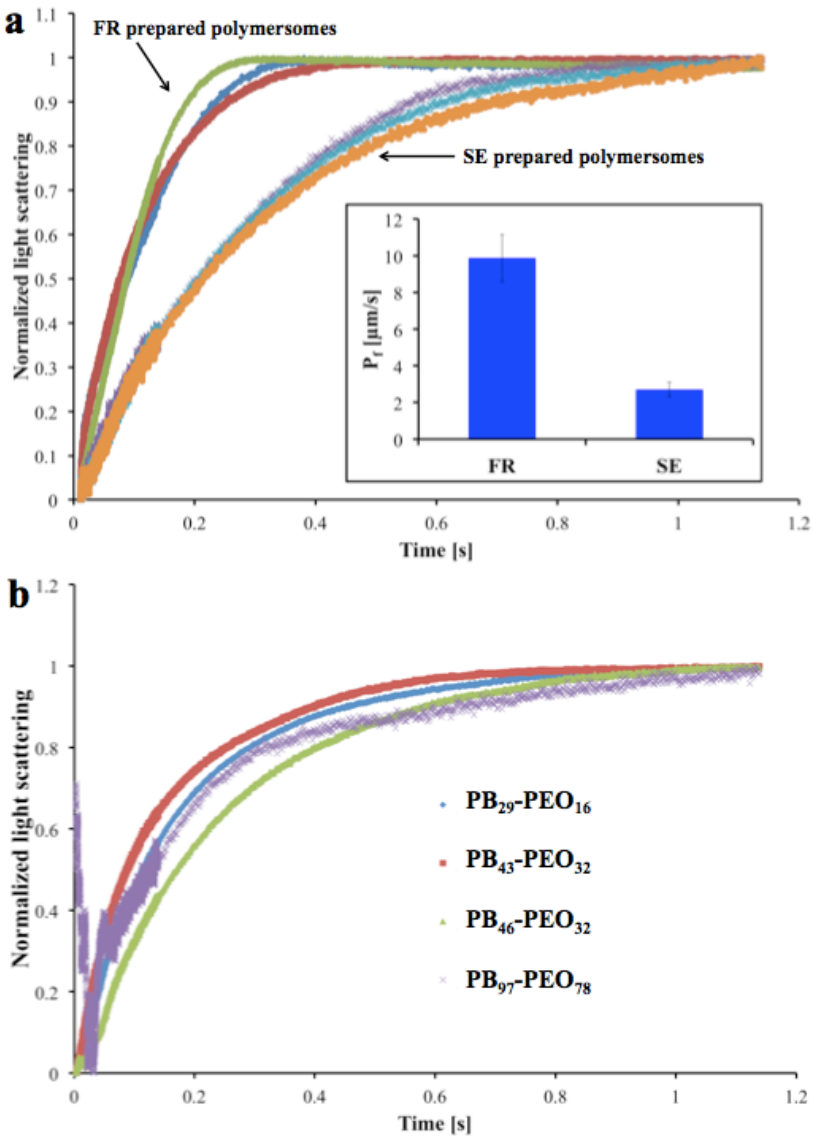

Figure 2: Influence of preparation method and M_n on bilayer response to osmotic shock. *a*) Light scattering of polymersomes polymersomes, prepared by DFR and SE as a function of time. *b*) Light scattering of SE prepared polymersomes of four polymers of different M_n. All curves were normalized to maximal scatter intensity value. 1 M NaCl was used as an osmotic agent. k was obtained by fitting the normalized curves to a single exponential function and P_f values were calulated using Equation 1.

In order to further analyze the properties of polymersomes in the extruded material, we measured the osmotic response by mixing polymersomes with 1 M NaCl and quantified vesicle shrinkage by SFLS. This served two purposes: to verify the existence of polymersomes

(as PB-PEO in our M_n range are known to be water-permeable[19,31,46]), and to quantify the polymersome osmotic water permeability P_f (Equation 1) - an important property when designing polymersomes for encapsulation applications. Only vesicular structures will respond to osmotic stress as micelles cannot shrink and a potential PEO swelling is too small to be detected by SFLS. Specifically we investigated DFR and SE prepared PB_{29}-PEO_{16} polymersomes. In order to get a reliable SFLS signal, polymersomes need to be monodisperse[47]. Thus, they need to be extruded prior to SFLS measurements. As far as DFR prepared polymersomes are known to be highly polydisperse also in a d_P range below 400 nm[43], extrusion were performed with 200nm pore size, where SE prepared polymersomes could only be extruded through 400 nm due to their lower apparent fluidity, as discussed above. This has to be kept in mind in the comparative analysis.

For both preparation methods polymersomes were detected with SFLS. P_f was three times higher with DFR prepared polymersomes than for SE prepared polymersomes (9.8±1.3 μm s^{-1} and 2.7±0.4 μm s^{-1} respectively), see Figure 2a). This difference could again be related to bilayer with lower apparent fluidity of the SE prepared polymersomes compared to the DFR prepared polymersomes. The softer membrane bilayers of DFR prepared polymersomes (which could be opened easier by extrusion) enable them to regulate their volume faster in response to a change in osmolarity. The difference in P_f is likely not due to density differences due to entanglement in the bilayer due to the small M_n of the polymer. P_f values are in agreement with values reported for PB-PEO polymersomes of comparable M_n[19,31,46]. Another reason for the difference could be the presence of remaining OG in the DFR prepared polymersomes or remaining organic solvent. Even though both have been removed using biobeads (for OG) and evaporation (for organic solvent), we cannot completely exclude small concentrations of detergent/solvent in the final sample.

The influence of M_n on polymersome bilayer response to osmotic shock was then determined using SE prepared polymersomes of all four polymers (Table 2), extruded through 400 nm pore size prior to SFLS measurements. For the determination of k the dead time of the instrument (0.7 ms) was not taken into account as the osmotic shrinkage kinetic range was $>$ 100 ms for all polymersome samples and therefore the influence of the first 0.7 ms is negligibly small. SFLS curves were comparable, see Figure 2b and all k values were in between 5.5 and

9.8 s^{-1}, however there was no correlation between k and M_n. The higher k compared to the SE prepared polymersomes of Figure 2a is due to the higher concentration used (10 mg/ml compared to 3 mg ml^{-1} in the DFR-SE comparison). In previous experiments we measured SLFS on DFR prepared PB-PEO polymersomes of polymers with M_n between 1.1 and 4 kg mol^{-1} [48]. Here, we observed decreasing k values with increasing M_n. Thus, the effect of M_n on k seems to be more pronounced for DFR than for SE prepared polymersomes. On the other hand, P_f is more than five times higher for the polymersomes from the two highest M_n polymers (17.4 and 17.13 μm s^{-1} for PB_{46}-PEO_{32} and PB_{97}-PEO_{78} polymersomes respectively) compared to polymersomes formed from the two lowest M_n polymers (3.75 and 3.58 μm s^{-1} for PB_{29}-PEO_{16} and PB_{43}-PEO_{32} polymersomes respectively). It is striking that the large permeability difference between PB_{43}-PEO_{32} and PB_{46}-PEO_{32} polymersomes occurs for a quite small change in M_n of 0.05 kg mol^{-1}. This will be further discussed in the next section. The noisy SFLS signal of PB_{97}-PEO_{78} polymersomes in Figure 2b is likely due to the high polydispersity of these after extrusion, as discussed in the previous section.

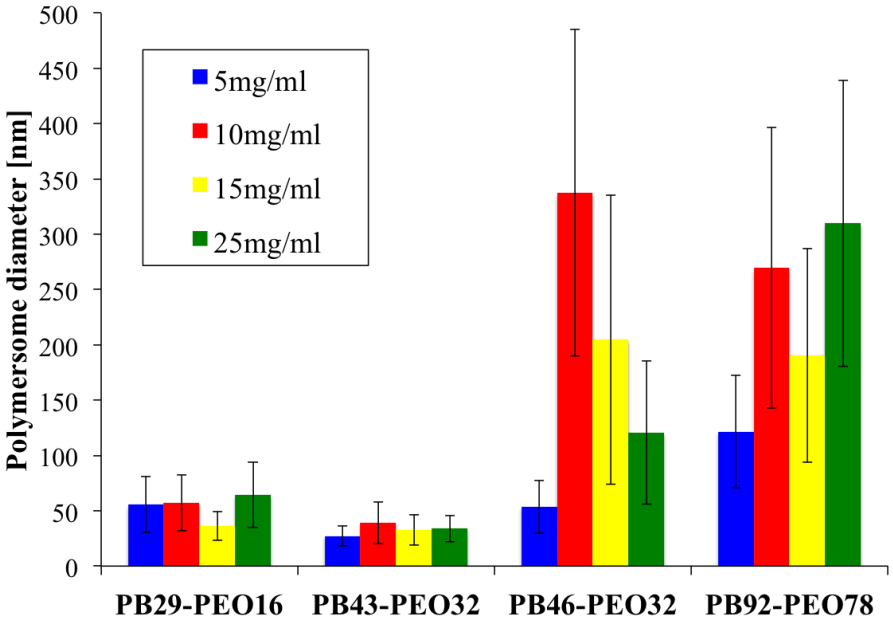

Figure 3: Comparison of SE prepared polymersomes of different concentrations followed by extrusion through 400 nm, measured via DLS. PB_{29}-PEO_{16} formed small monodisperse polymersomes, PB_{43}-PEO_{32} had high portions of micelles, where the last two revealed polydisperse polymersomes above 5 mg ml^{-1}.

Effect of concentration for SE formed polymersomes

In order to further analyze the effect of M_n and polymer concentration on the bilayer response to extrusion, we prepared polymersomes from the polymers listed in Table 2 with SE and extruded them at 400 nm due to the challenges with 200 nm pore size extrusion. Polymersomes were prepared from 5 mg ml^{-1}, 10 mg ml^{-1}, 15 mg ml^{-1} and 25 mg ml^{-1} concentration and size distributions were characterized by DLS.

For polymersomes of the two smallest polymers PB_{29}-PEO_{16} and PB_{43}-PEO_{32} $\langle d_P \rangle$ was < 60 nm for all concentrations, see Figure 3. This could indicate the presence of small non-vesicular structures. However the SFLS analysis clearly reveals that a least a significant portion of the PB_{29}-PEO_{16} and PB_{43}-PEO_{32} self-assembled morphologies are polymersomes. For polymersomes formed from the two largest polymers PB_{46}-PEO_{32} and PB_{97}-PEO_{78} $\langle d_P \rangle$ was > 100 nm at all concentrations except at 5 mg/mol PB_{46}-PEO_{32}. We previously observed an increase in $\langle d_P \rangle$ with increasing M_n for DFR prepared polymersomes[43] whereas other studies based on PB-PEO polymersomes do not report significant changes in $\langle d_P \rangle$ with increasing molecular weight[18].

The significant difference (mirroring the change in P_f discussed above) between PB_{43}-PEO_{32} and PB_{46}-PEO_{32} polymersomes is surprising, given the small difference in M_n between the two polymers. In our previous publication we also discussed the thermodynamic context of polymersome formation and found that there are regions, where the energy balance between the surface energy and bending energy of a polymer bilayer sheet displays one global energetic minimum, leading to more monodisperse polymersomes, or several local minima, resulting in both, monodisperse or polydisperse polymersomes[43]. In the region of the PB_{43}-PEO_{32} and PB_{46}-PEO_{32} (f 0.25-0.35, M_n 2-5 kg mol^{-1}) the latter energetic balance is dominant. This could explain the large difference in $\langle d_P \rangle$. Another potential explanation of the difference could be that PB_{43}-PEO_{32} was synthesized following a two-step approach, starting with EO-endcapped PB[42], whereas PB_{46}-PEO_{32} was synthesized after a one-step-approach[41]. However, both synthesis products exhibited a narrow size distribution as measured with SEC and NMR (see supplementary information). Since different solubilities of PB and PEO in THF could result in slightly different elution times at higher content

of PEO at SEC, we only used NMR-derived M_n. PB_{43}-PEO_{32} had a minor fraction of small M_n impurities, but the effect of this impurity does not appear as a satisfactory explanation for the difference in d_P of the extruded polymersomes.

Taken together, these results show that polymer concentration does not seem to have a major impact on polymersome size after extrusion. The only exception being PB_{46}-PEO_{32} where the change from 5 to 10 mg ml^{-1} resulted in a large change in $\langle d_P \rangle$ from around 60 nm to 350 nm.

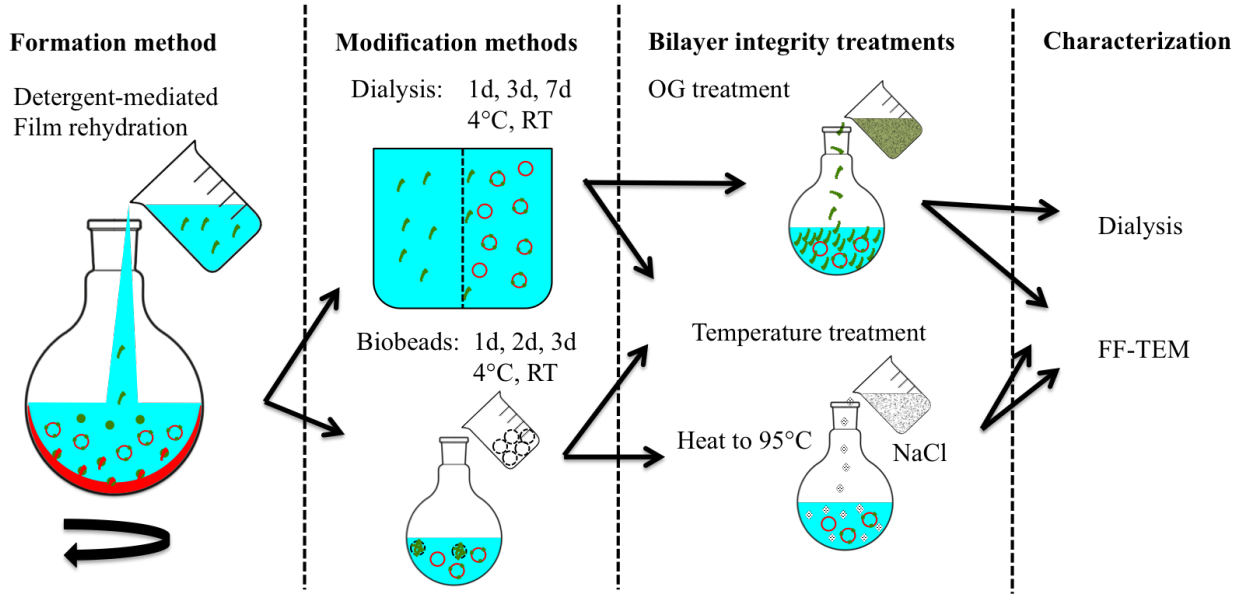

Figure 4: Schematic overview of the third part of this paper, dealing with detergent removal. After polymersome formation via detergent-mediated film rehydration, the polymersomes where either modified using dialysis or biobead addition. For integrity tests samples were collected and subjected to either an excess of the detergent OG (OGST) or high temperature, combined with NaCl (TSST). Subsequent structural characterization was performed using DLS and FF-TEM.

Bilayer response to detergent removal

An important issue in polymersome formulations is the issue of detergents. For example in order to produce polymersomes with reconstituted functional membrane proteins it is necessary to remove the detergent used to stabilize the protein[14].

Here we analyze OG detergent removal (starting concentration 2.6 mg ml^{-1}) from DFR prepared polymersomes of PB_{29}-PEO_{16} (as far as there is no detergent involved in SE), using dialysis and biobeads. Both methods were applied under varying time and temperature conditions. Dialysis was performed for 1 d, 3 d and 7 d at 4°C and 22°C. Biobeads were exposed to the sample for 1 d, 2 d and 3 d at the same temperatures. Samples were exposed to two stress tests: OG stress test (OGST) consisting of exposure to excess (85 mg/ml) OG; Temperature and salt test (TSST), consisting of NaCl addition to a final concentration of 500 mM combined with heating to 95°C, for an overview see Figure 4. From this procedure, a stability threshold was deduced from DLS analysis of the sample from 3 d dialysis at 4°C after treatment of several temperature steps and OG concentrations steps. Originally, only T treatment without the addition of NaCl was planned, but surprisingly the polymersomes remained unchanged even at 95°C, so different amounts of NaCl had to be added to finally break them between 500 mM and 1M. The threshold was then chosen to be 95°C and 500 mM NaCl (meaning adding 450 mM NaCl to the already existing 50 mM NaCl of the buffer). The same was done with addition of OG. 100 mg ml^{-1} OG was known to result in complete dissolution of polymersomes[19]. The representative sample broke down between 80 mg/ml and 90 mg/ml OG leading to choose 85 mg/ml OG for the integrity test.

The more detergent remaining in the bilayer, the easier detergent molecules can convert the polymersomes to mixed micelles[49]. Thus, decreased d_P at same OG (detergent) treatment is an indication of the modification and its parameter being less effective at removing detergent from the bilayer.

Dialysis detergent removal

OG was dialyzed out from 1-7 d at 22°C and 4°C. Neither OGST nor TSST resulted in significant changes in $\langle d_P \rangle$ as measured per DLS and FF-TEM, see Figure 5. The discrepancies between $\langle d_P \rangle$ values obtained using DLS and FF-TEM at the OGST samples is likely due to OG-induced aggregation of structures[28]. From the FF-TEM micrographs, several aggregated polymersomes and micelles can be observed and classified manually. However with DLS, large aggregates would be classified as large polymersomes. For TSST, where there is less aggregation, the differences in $\langle d_P \rangle$ are smaller. TSST revealed to be the more

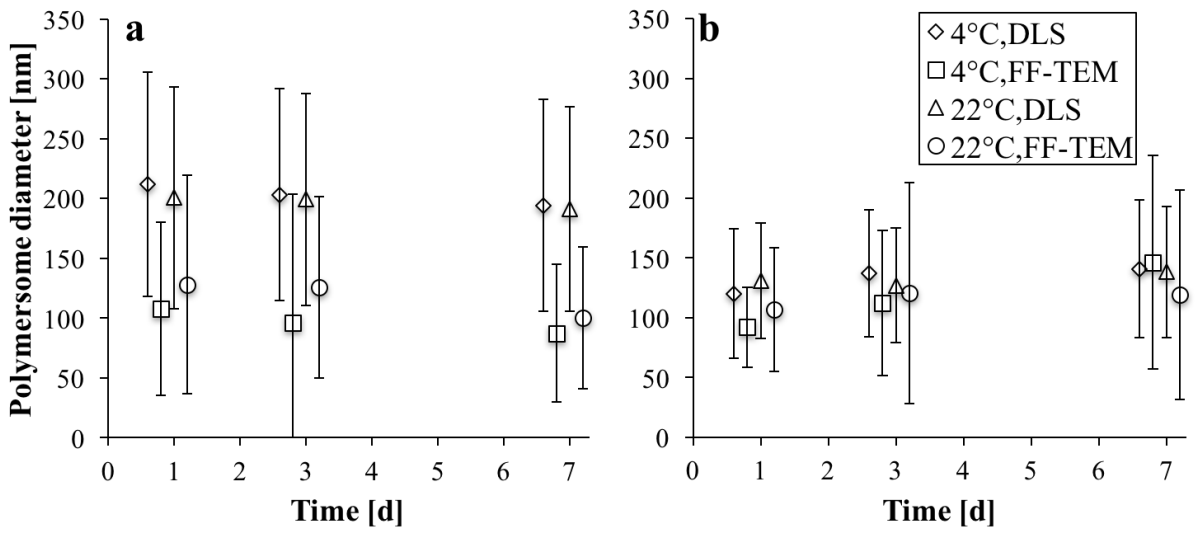

Figure 5: Comparison of $\langle d_P \rangle$ of samples after OGST and TSST following dialysis for 1 d, 3 d and 7 d at 4°C and 22°C as measured by DLS and FF-TEM. (a) OGST. (b) TSST. Data points are slightly shifted in time for better visualization, however each cluster refers to 1 d, 3 d and 7 d respectively. Error bars represent δ in the case of DLS measurements and standard deviation in the case for FF-TEM measurements.

reliable stress test, concerning detergent removal with dialysis.

Visual inspection of the FF-TEM images revealed more intact polymersomes after 1 d at 22°C after TSST (Figure 6a+b) compared to 1 d dialysis at 4°C (Figure 6c+d). These polymersomes appeared as untreated polymersomes[43], where the 4°C dialyzed polymersomes had a collapsed appearance that also made it harder to fracture them for FF-TEM. After 3 d dialysis at 22°C and TSST, the polymersome sturdiness was comparable but there were more polymersomes than at 4°C. Finally, dialysis at 7 d, 22°C & TSST (Figure 6e+f) revealed slightly more multilamellar polymersomes than dialyzed samples at 7 d, 4°C (Figure 6g) or samples that were treated with biobeads for 3 d at both temperatures (4°C see Figure 6h). The right large polymersome in Figure 6e is clearly multilamellar, whereas the large one at the bottom of Figure 6f could also be multivesicular. This is noteworthy for polymersome production for some applications (e.g. drug delivery vesicles) multilamellar vesicles should be avoided.

The finding of multilamellar polymersomes after dialysis is in contrast to findings from

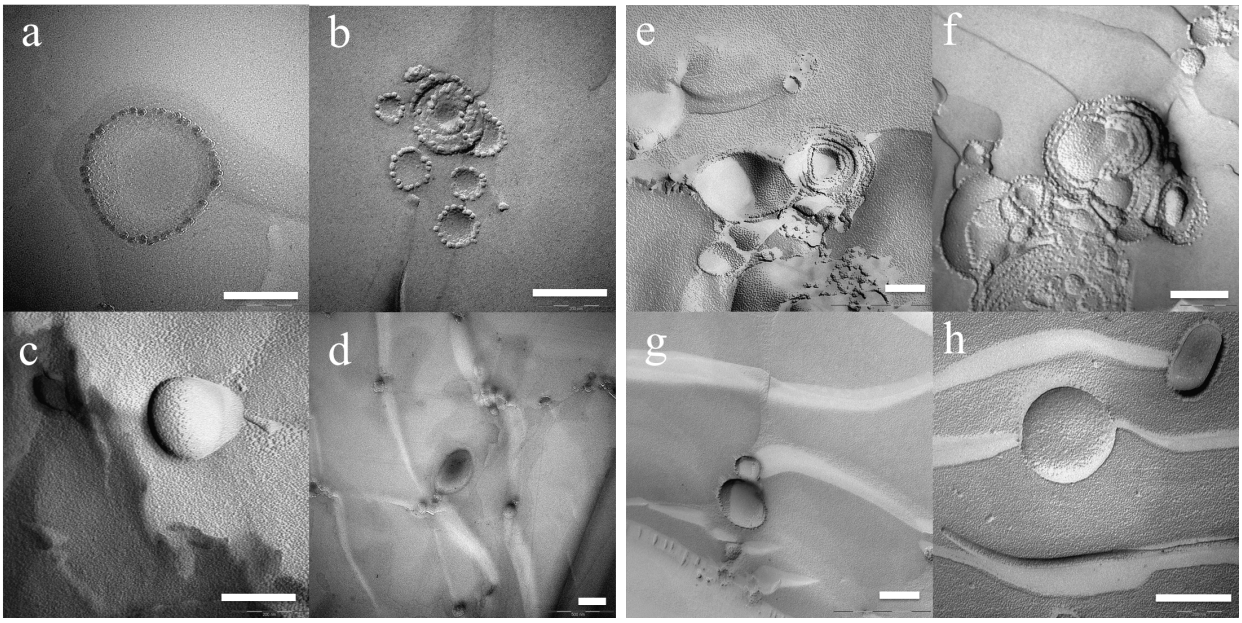

Figure 6: FF-TEM images of a)+b) polymersomes after 1 d dialysis at 4°C and c)+d) at 22°C, e)+f) after 7 d dialysis at 22°C, g) at 4°C and h) after 3d of biobead removal at 4°C, all followed by TSST. Polymersomes from 4°C dialysis had a more collapsed and ruptured appearance compared to polymersomes dialyzed at 22°C. There were multilamellar polymersomes observed at 22°C dialysis, where 4°C dialysis and biobead removal led to mainly unilamellar polymersomes. Scale bar is 200 nm.

the liposome literature where dialysis is presented as an ideal tool for unilamellar vesicles[17,50] although Rhoden et al. did observe a minor appearance of multilamellar liposomes[50]. Multilamellar polymersomes were also in minority, when compared to untreated polymersomes after 2 d biobeads detergent removal[43]. Thus, if using dialysis during polymersome production, an extra step may be required to achieve unilamellar polymersomes.

Taken together these findings reveal that there was no significant change in polymersome morphology upon changing the investigated parameters in dialysis-based detergent removal.

Biobeads detergent removal

The polymersome solutions were exposed to 22 mg biobeads per ml solution. This should be sufficient to remove the major fraction of detergent as far as they have a OG adsorptive

capacity of 117 mg g^{-1} [14], which would result in 2.57 mg adsorption capacity for the 22 mg biobeads added (starting OG concentration 2.6 mg ml^{-1}). In terms of exposure time, no data on detergent removal rates have been published for polymesomes. Discher et al. showed that detergent-polymersome interaction is qualitatively and quantitatively different from detergent-liposome interactions[49]. For liposomes, 1 d exposure is usually sufficient to ensure efficient removal thus we exposed polymersomes to biobeads for up to 3 d to ensure sufficient removal. We did not exceed 3 d as long exposure times could potentially lead to polymer adsorption by the biobeads. Polymers are likely adsorbed with a higher affinity than lipids, as far as their hydrophobic tails are longer. Lipids are adsorbed by biobeads with only 1 mg g^{-1} biobeads (thus 117 times lower than their main target - detergents)[14].

Neither FF-TEM nor DLS size distribution did reveal any significant change of $\langle d_P \rangle$ between day 1, 2 and 3, for any of the treatments (OGST and TSST at 4°C or 22°C) (Figure 7a for OGST and b for TSST). A higher detergent absorption rate with increased temperature, as reported for liposomes from Levy[15] was not found for polymersomes. Polymer adsorption did not seem play a major role with 3 d biobeads exposure.

In conclusion there was no significant changes in polymersome morphology for the investigated parameters during biobead detergent removal.

CONCLUSIONS

This study investigated polymersome formation and modification with a focus on their influence of the physical properties of the outcoming polymersomes. We investigated two polymersome formation methods, four polymers of different M_n and polymersomes of four different concentrations for their influence in terms of poylmersome response to extrusion, osmotic shock and detergent removal by dialysis and biobeads addition.

DFR prepared polymersomes are more leaky but also have a higher apparent fluidity than SE prepared polymersomes. There seems to be a threshold for SE prepared polymersomes between 3.75 kg mol^{-1} (PB_{43}-PEO_{32}) and 3.8 kg mol^{-1} (PB_{46}-PEO_{32}). Thus for PB_{43}-PEO_{32} and PB_{29}-PEO_{16} the bilayer has a lower apparent fluidity and break down to polymersomes with d_P of 50 nm and smaller non-vesicular structures. For PB_{46}-PEO_{32} and PB_{92}-PEO_{78}

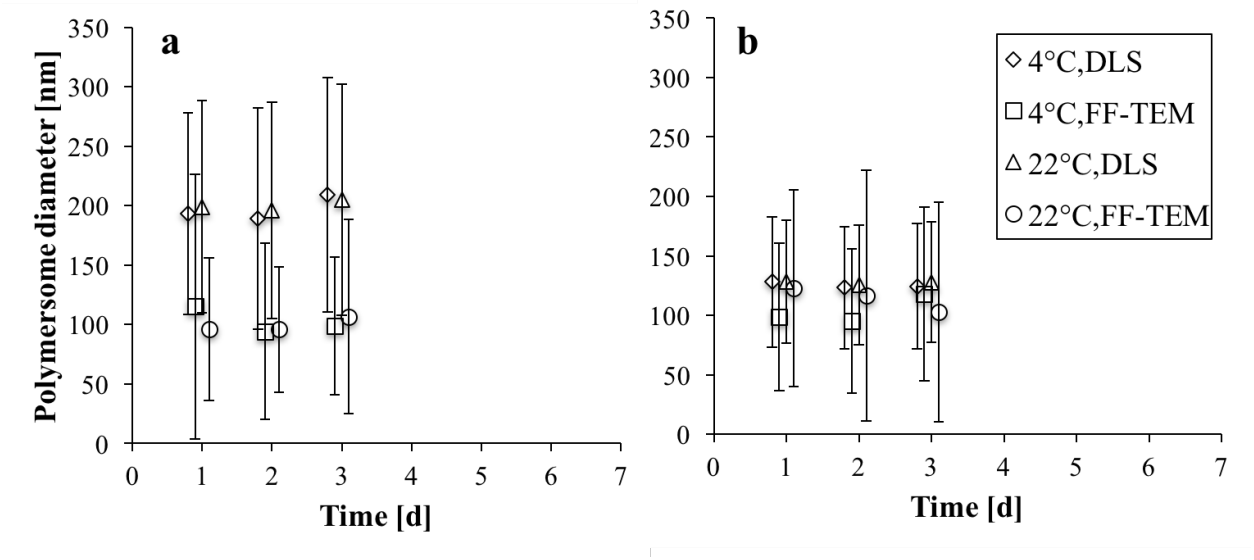

Figure 7: Comparison of $\langle d_P \rangle$ of biobeads detergent removal samples for 1 d, 2 d and 3 d at 4°C and 22°C with a) subsequent OGST and b) TSST, measured with DLS and FF-TEM. Data points are slightly shifted in time for better visualization, however each cluster refers to 1 d, 2 d and 3 d respectively. Error bars represent δ for DLS measurements and standard deviation for FF-TEM measurements. There was no significant change in $\langle d_P \rangle$.

polymersomes of d_P 200-300 nm at PB_{46}-PEO_{32} were observed. At 5 mg ml^{-1} polymer concentration the majority of SE prepared polymersomes broke down to smaller structures, where at 10, 20 and 25 mg ml^{-1} $\langle d_P \rangle$ remained between 200-300 nm in the case of the polymers $> M_n$ 3.8 kg mol^{-1}. The extrusion stability threshold between 3.75 kg mol^{-1} and 3.8 kg mol^{-1} is also reflected in the bilayer response to osmotic shock, where there is a five times increase in permeability going from PB_{43}-PEO_{32} to PB_{46}-PEO_{32}. Regarding the bilayer response to detergent removal by dialysis and biobeads, there were no significant differences in bilayer response to OGST and TSST between the varying parameters (4°C and 22°C or 1 d, 3 d, and 7 d for dialysis and 1, 2 or 3 d at biobeads). Taken together our results provide a step towards biocompatible polymersome formation and modification which can facilitate biomolecule incorporation for applications relying on biomimetic membrane technology.

ACKNOWLEDGMENTS

We thank Lars Schulte and Simon Levinsen, DTU Nanotech for assistance with the polymer synthesis; Fadoua Sbai, Aquaporin A/S, for assistance with SFLS analysis and Klaus Qvortrup and Ramon Liebrechts, University of Copenhagen, for providing assistance with freeze fracture and access to the Leica freeze fracture instruments. JH was supported by an industrial PhD grant from Innovation Fund Denmark. CHN was supported by the IBISS - Industrial Biomimetic Sensing and separation platform (http://www.ibiss.dtu.dk) funded by the Danish Innovation Fund Grant no. 097-2012-4.

ABBREVIATIONS / NOMENCLATURE

Bd - 1,3-Butadiene

n-BuLi - n-Butyl lithium

n-Bu_2Mg - n-Dibutylmagnesium

DFR - Detergent-mediated film rehydration

DLS - Dynamic light scattering

EO - Ethylene oxide

f - Hydrophilic volume ratio

FR - Film rehydration

HPLC - High performance liquid chromatography

M_n - Number-averaged molecular weight

NNLS - Non-negatively constrained least squares

OG - n-Octyl-β-D-Glucopyranoside

OGST - OG stress test

P2VP - Poly(2-vinylpyridine-b-ethyleneglycol)

PB - 1,2-Polybutadiene

PBO - Polybutylene oxide

PDI - Polydispersity index of the polymer length, defined as M_w/M_n

PDMS - Polydimethylsiloxane

PEE - Polyethylethylene

PEO - Polyethylene oxide

PIAT - Poly-L-isocyanoalanine(2-thiophen-3-yl-ethyl) amide

PLA - Poly(lactic acid)

PMOXA - Polymethyloxazoline

PS - Polystyrene

SE - Solvent evaporation

SEC - Size exclusion chromatography

SFLS - Stopped-flow light scattering

tBuP4 - 1-*tert*-Butyl-4,4,4-Tris(dimethylamino)-2,2-bis[Tris(dimethyl-amino) -phosphoranylidenamino]-$2\lambda^5$,$4\lambda^5$-catenadi(phosphazene)

FF-TEM - Freeze fracture with transmission electron microscopy observation

THF - Tetrahydrofuran

TSST - Temperature and salt stress test

References

1. J. Nicolas, S. Mura, D. Brambilla, N. Mackiewicz, and P. Couvreur, Chem. Soc. Rev. **42**, 1147 (2013).

2. J. Yang, H. Liu, and X. Zhang, Biotechnol. Adv. **32**, 804 (2014).

3. K. Langowska, C. G. Palivan, and W. P. Meier, Chem. Commun. **49**, 128 (2013).

4. P. V. Pawar, S. V. Gohil, J. P. Jain, and N. Kumar, Polym. Chem. **4**, 3160 (2013).

5. R. Langer, Science **249**, 1527 (1990).

6. C. Hélix-Nielsen, Anal. Bioanal. Chem. **395**, 697 (2009).

7. Nanyang Technological University, Aquaporin AS, C. Y. Tang, C. Qiu, Y. Zhao, W. Shen, A. Vararattanavech, R. Wang, X. Hu, J. Torres, et al., *Aquaporin based thin film composite membranes*, WIPO (2013).

8. C. Y. Tang, Y. Zhao, R. Wang, C. Hélix-Nielsen, and A. G. Fane, Desalination **308**, 34 (2013).

9. P. S. Zhong, T.-S. Chung, K. Jeyaseelan, and A. Armugam, J. Membr. Sci. **407-408**, 27 (2012).

10. H. L. Wang, T.-S. Chung, Y. W. Tong, K. Jeyaseelan, A. Armugam, H. H. P. Duong, F. Fu, H. Seah, J. Yang, and M. Hong, J. Membr. Sci. **434**, 130 (2013).

11. L. A. Bagatolli, T. Parasassi, and E. Gratton, Chem. Phys. Lipids **105**, 135 (2000).

12. D. E. Discher and A. Eisenberg, Science **297**, 967 (2002).

13. S. Morandat and K. El Kirat, Colloids Surf. B: Biointerfaces **55**, 179 (2007).

14. J.-L. Rigaud, D. Levy, G. Mosser, and O. Lambert, Eur. Biophys. J. **27**, 305 (1998).

15. D. Levy, A. Bluzat, M. Seigneuret, and J.-L. Rigaud, Biochim. Biophys. Acta - Biomembr. **1025**, 179 (1990).

16. J. Philippot, S. Mutaftschiev, and J. P. Liautard, Biochim. Biophys. Acta - Biomembr. **734**, 137 (1983).

17. O. Zumbuehl and H. G. Weder, Biochim. Biophys. Acta **640**, 252 (1981).

18. H. Marsden, C. Quer, E. Sanchez, L. Gabrielli, W. Jiskoot, and A. Kros, Biomacromolecules **11**, 833 (2010).

19. M. Kumar, J. Habel, Y.-x. Shen, W. P. Meier, and T. Walz, J. Am. Chem. Soc **134**, 18631 (2012).

20. K. Saegusa and F. Ishii, Langmuir **18**, 5984 (2002).

21. K. Kita-Tokarczyk, J. Grumelard, T. Haefele, and W. P. Meier, Polymer **46**, 3540 (2005).

22. J. A. Jackman, Z. Zhao, V. P. Zhdanov, C. W. Frank, and N.-J. Cho, Langmuir **30**, 2152 (2014).

23. C. Lopresti, H. Lomas, M. Massignani, T. Smart, and G. Battaglia, J. Mater. Chem. **19**, 3557 (2009).

24. T. C. Kaufmann, A. Engel, and H.-W. Rémigy, Biophys. J. **90**, 310 (2006).

25. M. Kumar, M. Grzelakowski, J. Zilles, M. M. Clark, and W. P. Meier, Proc. Natl. Acad. Sci. USA **104**, 20719 (2007).

26. M. Borgnia, D. Kozono, G. Calamita, P. Maloney, and P. Agre, J. Mol. Biol. **291**, 1169 (1999).

27. H. Shen and A. Eisenberg, J. Phys. Chem. B **103**, 9473 (1999).

28. U. Kragh-Hansen, M. le Maire, and J. V. Møller, Biophys. J. **75**, 2932 (1998).

29. J. Lee, H. Bermudez, B. M. Discher, M. Sheehan, Y.-Y. Won, F. S. Bates, and D. E. Discher, Biotechnol. Bioeng. **73**, 135 (2001).

30. J. R. Howse, R. A. L. Jones, G. Battaglia, R. E. Ducker, G. J. Leggett, and A. J. Ryan, Nat. Mater. **8**, 507 (2009).

31. B. M. Discher, Y.-Y. Won, D. Ege, J. Lee, F. S. Bates, D. E. Discher, and D. Hammer, Science **284**, 1143 (1999).

32. Z. Fu, M. A. Ochsner, H.-P. M. De Hoog, N. Tomczak, and M. Nallani, Chem. Commun. **47**, 2862 (2011).

33. S. Hauschild, U. Lipprandt, A. Rumplecker, U. Borchert, A. Rank, R. Schubert, and S. Förster, Small **1**, 1177 (2005).

34. A. Akbarzadeh, R. Rezaei-Sadabady, S. Davaran, S. W. Joo, N. Zarghami, Y. Hanifehpour, M. Samiei, M. Kouhi, and K. Nejati-Koshki, Nanoscale Res. Lett. **8**, 102 (2013).

35. J. Thiele, A. R. Abate, H. C. Shum, S. Bachtler, S. Förster, and D. A. Weitz, Small **6**, 1723 (2010).

36. J. Thiele, D. Steinhauser, T. Pfohl, and S. Förster, Langmuir **26**, 6860 (2010).

37. S. M. Christensen and D. Stamou, in *Springer* (Springer, Dordrecht, The Netherlands, 2011), pp. 87–112.

38. A. Seddon, P. Curnow, and P. J. Booth, Biochim. Biophys. Acta - Biomembr. **1666**, 105 (2004).

39. N.-J. Cho, L. Hwang, J. Solandt, and C. Frank, Materials **6**, 3294 (2013).

40. F. Szoka and D. Papahadjopoulos, Proc. Natl. Acad. Sci. USA **75**, 4194 (1978).

41. S. Förster and E. Krämer, Macromolecules **32**, 2783 (1999).

42. M. A. Hillmyer and F. S. Bates, Macromolecules **29**, 6994 (1996).

43. J. Habel, A. Ogbonna, N. Larsen, L. Schulte, K. Almdal, and C. Hélix-Nielsen, J. Polym. Sci. B Polym. Phys. pp. n/a–n/a (2015).

44. B. Coldren, R. van Zanten, M. J. Mackel, J. A. Zasadzinski, and H.-T. Jung, Langmuir **19**, 5632 (2003).

45. S. Jain, X. Gong, L. Scriven, and F. S. Bates, Phys. Rev. Lett. **96**, 138304 (2006).

46. A. Carlsen, N. Glaser, J.-F. Le Meins, and S. Lecommandoux, Langmuir **27**, 4884 (2011).

47. M. Grzelakowski, M. F. Cherenet, Y.-x. Shen, and M. Kumar, J. Membr. Sci. **479**, 223 (2015).

48. J. Habel, Tech. Rep., Copenhagen, Denmark (2011).

49. V. Pata, F. Ahmed, D. E. Discher, and N. Dan, Langmuir **20**, 3888 (2004).

50. V. Rhoden and S. M. Goldin, Biochemistry-US **18**, 4173 (1979).